Synthetic and Systems Biotechnology 10 (2025) 707–718

Contents lists available at ScienceDirect

Synthetic and Systems Biotechnology

journal homepage: www.keaipublishing.com/en/journals/synthetic-and-systems-biotechnology

Original Research Article

Enhanced chlorogenic acid production from glucose via systematic metabolic engineering of *Saccharomyces cerevisiae*

Shuai Tu, Junjie Wang, Pengming Yang, Yan He, Zhixing Gong, Weihong Zhong *

College of Biotechnology and Bioengineering, Zhejiang University of Technology, Hangzhou, 310014, China

ARTICLE INFO

Keywords:
Chlorogenic acid
Saccharomyces cerevisiae
Systematic metabolic engineering
PEP and E4P
Fermentation conditions

ABSTRACT

Chlorogenic acid (CGA) is a valuable phenolic acid with various pharmaceutical functions. In our previous study, *de novo* synthesis of CGA in *Saccharomyces cerevisiae* was achieved. However, its yield required improvement before large scale production. In this study, systematic metabolic engineering strategy was used to reconstruct chassis cell *S. cerevisiae* YC0707 to enhance its CGA yield from glucose. To balance the supply of phosphoenolpyruvate (PEP) and erythrose 4-phosphate (E4P), *ZWF1* (encoding glucose-6-phosphate dehydrogenase) and *GND1* (encoding 6-phosphogluconate dehydrogenase) were overexpressed by strong promoter P_{TEF1} swapping, thereby strengthening the pentose phosphate pathway. The mutant of phosphofructokinase ($PFK2^{S718D}$) was further introduced to weaken the glycolytic pathway. Then, the *p*-coumaric acid synthesis capacity was enhanced by employing tyrosine ammonia lyase from *Rhodotorula glutinis* (RgTAL), ΔHAM1, and ΔYJL028W. Fusion expression of AtC4H (cinnamate-4-hydroxylase) and At4CL1 (4-coumarate CoA ligase 1), together with CsHQT (hydroxycinnamoyl CoA quinate transferase) and AtC3′H (*p*-coumaroyl shikimate 3-hydroxylase), improved biosynthetic flux to CGA. Subsequently, the microenvironment of P450 enzymes was improved by overexpressing *INO2* (a transcription factor for lipid biosynthesis) and removal of heme oxygenase gene *HMX1*. Furthermore, screening potential transporters to facilitate CGA accumulation. Finally, we optimized the fermentation conditions. Using these strategies, CGA titers increased from 234.8 mg/L to 837.2 mg/L in shake flasks and reached 1.62 g/L in a 5-L bioreactor, representing the highest report in *S. cerevisiae* and providing new insights for CGA production.

1. Introduction

Chlorogenic acid (CGA, 3-*O*-caffeoylquinic acid) is a phenylacrylate polyphenol compound produced *via* the shikimic acid pathway in plants [1]. CGA has been increasingly utilized in the cosmetics, nutrition, and pharmaceutical industries due to its broad range of activities, including anti-inflammatory [2], anti-tumor [3], antibacterial [4], and immunomodulatory effects [5]. Moreover, CGA plays an important role in skin whitening and rejuvenation due to its antioxidant properties [6]. Traditionally, commercial production of CGA has relied on extraction from natural plants, which faces challenges with low extraction efficiency, lengthy growth cycles, and adverse environmental impacts [1]. Therefore, it's prospective to develop high-efficiency and sustainable methods for synthesizing CGA using microbial cell factories.

The biosynthesis of CGA involves several direct precursors: *p*-coumaroyl-CoA or caffeoyl-CoA and quinic acid. This synthetic pathway requires heterogeneous enzymes, including hydroxycinnamoyl-CoA quinate transferase (HQT) and *p*-coumaroyl shikimate 3-hydroxylase (C3′H) [7,8]. *p*-Coumaroyl-CoA and caffeoyl-CoA are generated from *p*-coumaric acid and caffeic acid by 4-coumarate CoA ligase (4CL) [9]. Therefore, the availability of *p*-coumaric acid or caffeic acid, along with quinic acid, is crucial for CGA biosynthesis. However, 4CL preferentially catalyzes *p*-coumaric acid to *p*-coumaroyl-CoA when both *p*-coumaric acid and caffeic acid are all present in *Saccharomyces cerevisiae* [10].

Several reports have achieved the biosynthesis of CGA in microorganisms, with its biosynthetic pathway successfully reconstituted in *Escherichia coli* and *S. cerevisiae*. In *E. coli*, the CGA titer reached 450 mg/L by deleting the 3-dehydroquinate dehydratase (AroD) and overexpressing the quinate dehydrogenase (YdiB), combined with the supplementation of caffeic acid [11]. A cell-free biosynthetic system increased the CGA titer to 711.26 mg/L through chassis-cell extractions and purified Spy cyclase mixtures [12]. An authentic polyculture system

Peer review under the responsibility of Editorial Board of Synthetic and Systems Biotechnology.
* Corresponding author.
E-mail address: whzhong@zjut.edu.cn (W. Zhong).

https://doi.org/10.1016/j.synbio.2025.03.004
Received 30 October 2024; Received in revised form 15 February 2025; Accepted 5 March 2025
Available online 20 March 2025

for *de novo* CGA biosynthesis was designed, consisting of three *Escherichia coli* strain modules: one producing CA, another producing QA, and a third converting these precursors to QA, resulting in a CGA titer of 78 mg/L [13]. In addition, CGA titers of 638.2 mg/L in shake-flask cultures and 2789.2 mg/L in a 5-L fermenter were achieved by modular pathway optimization, cofactor engineering, and rational design of YdiB in *E. coli* [14]. In *S. cerevisiae,* the CGA biosynthetic pathway was reconstituted, realizing a CGA yield of 806.8 mg/L in a 1-L bioreactor and 234.8 mg/L in shake-flask cultures *via* unlocking the shikimate pathway and optimizing carbon distribution, optimizing the L-Phe branch, and adjusting the copy number of CGA pathway genes [15]. Overall, *S. cerevisiae* is widely utilized for the biosynthesis of phenolic acids due to its versatile genetic engineering tools [16], efficient expression of cytochrome P450 enzymes [17], and stabilization of scale-up fermentation [18]. Therefore, *S. cerevisiae* is considered a suitable chassis for the *de novo* biosynthesis of CGA.

Although progress has been made in *de novo* biosynthesis of CGA, the production of CGA still faces several challenges in *S. cerevisiae*. Since phosphoenolpyruvate (PEP) and erythrose-4-phosphate (E4P) directly connect central carbon metabolism to aromatic compounds biosynthetic pathway [19]. Optimizing the supply of PEP and E4P to the shikimate through modifications in central carbon metabolism produced 13 mM of 2-phenylethanol [20]. Heterologous expression of P450 enzymes from plants or other species may result in insufficient cofactor supply and rate-limiting steps for plant natural product synthesis in yeast [21]. Therefore, a suitable microenvironment for P450 expression is essential for microbial cell factories producing phenolic acids [22,23]. For instance, engineering cofactor supply and recycling achieved the caffeic acid titer to 5.5 g/L in *S. cerevisiae* [24]. The yield of diterpenoids reached 67.69 mg/L through engineering the microenvironment of P450s in *S. cerevisiae* [25]. Furthermore, the supply of synthetic precursors, such as *p*-coumaric acid and quinic acid, is essential for increasing CGA production [26]. Although strategies to enhance the production of aromatic compounds in *S. cerevisiae* are well-established, the studies on the conversion of these precursors to CGA are limited.

In this study, a systematic metabolic engineering strategy was utilized to address the aforementioned challenges for high production of CGA from glucose in *S. cerevisiae* (Fig. 1). In phase I, the PPP pathway

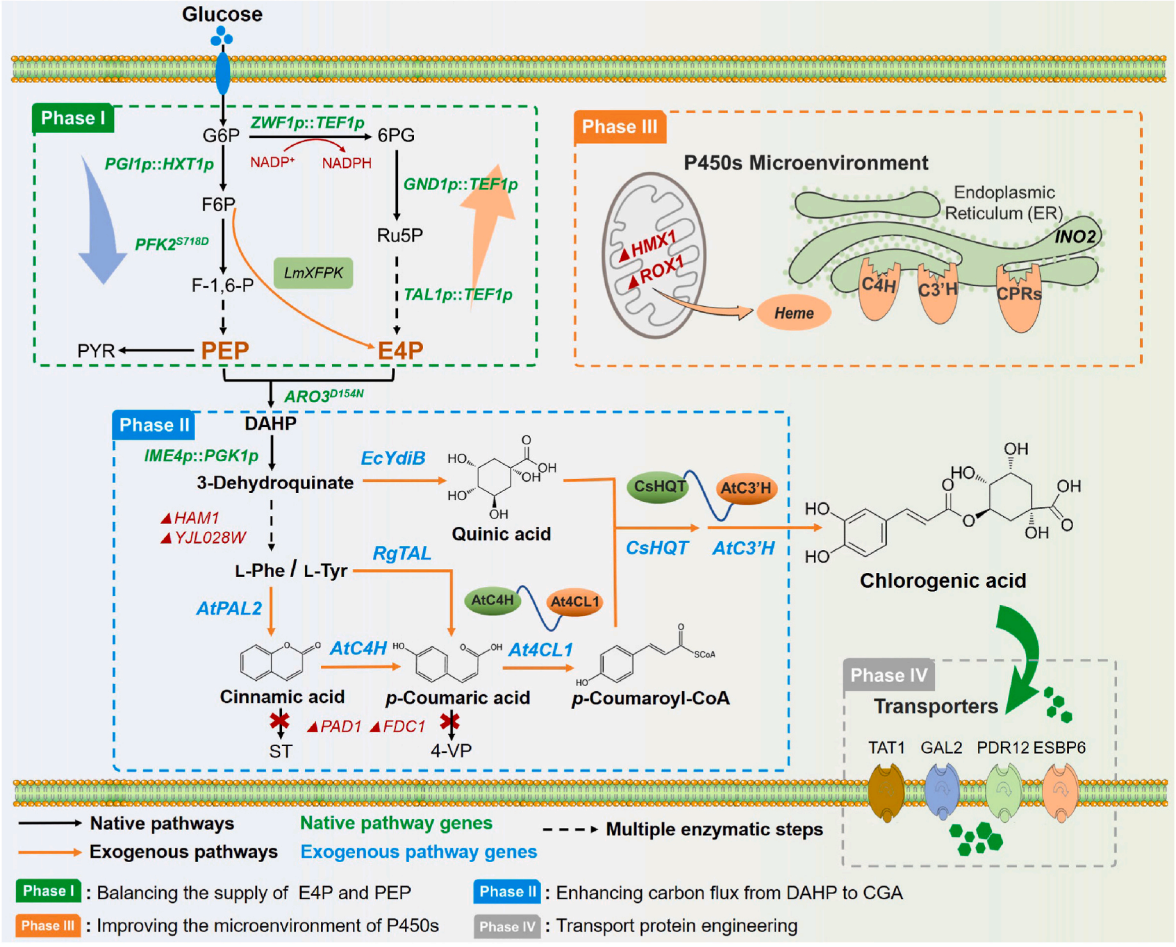

Fig. 1. Systematic metabolic engineering for the *de novo* biosynthesis of chlorogenic acid in *S. cerevisiae*. Phase I: Balancing the supply of E4P and PEP; Phase II: Enhancing carbon flux from DAHP to CGA; Phase III: Improving the microenvironment of P450s; Phase IV: Transport protein engineering. G6P, glucose-6-phosphate; F6P, fructose-6-phosphate; 6 PG, 6-phosphogluconic acid; Ru5P, ribulose-5-phosphate; F-1,6-P, fructose-1,6-bisphosphate; PEP, phosphoenolpyruvate; E4P, erythose-4-phosphate; PYR, pyruvate; DAHP, 3-deoxy-arabino-heptulosonate-7-phosphate; L-Phe, L-phenylalanine; L-Tyr, L-tyrosine; ST, styrene; 4-VP: 4-vinylphenol. Endogenous pathway gene: PGI1, phosphoglucose isomerase; ZWF1, glucose-6-phosphate dehydrogenase; GND1, 6-phosphogluconate dehydrogenase; TAL, transaldolase; PFK2^{S718D}, phosphofructokinase mutant; IME4, mRNA N6-adenosine methyltransferase; ARO3^{D154N}, L-phenylalanine feedback-insensitive chorismate mutase; HAM1, nucleoside triphosphate pyrophosphohydrolase; YJL028W, protein of unknown function; FDC1: ferulic acid decarboxylase; PAD1: phenylacrylic acid decarboxylase; HMX1, heme oxygenase; ROX1, heme-dependent repressor of hypoxic genes; INO2, a transcription factor for lipid biosynthesis; CPRs, P450 reductases; TAT1, tyrosine and tryptophan amino acid transporter; GAL2, galactose permease; PDR12 and ESBP6, transporters of increasing tolerance to aromatic acids. Heterologous genes: LmXFPK, phosphoketolase; AtPAL2, phenylalanine ammonia lyase 2; RgTAL, tyrosine ammonia lyase; AtC4H, cinnamate-4-hydroxylase; At4CL1, 4-coumarate CoA ligase 1; EcYdiB, quinate dehydrogenase; CsHQT, hydroxycinnamoyl-CoA quinate transferase; AtC3′H, *p*-coumaroyl shikimate 3-hydroxylase.

strengthening coupled with the EMP pathway weakening was designed to balance the supply of E4P and PEP. In phase II, optimizing the *p*-coumaric acid pathway and fusion expression of AtC4H and At4CL1, together with CsHQT and AtC3′H for enhancing carbon flux from DAHP to CGA. In phase III, improving the microenvironment of P450s by overexpressing *INO2* and deleting *HMX1*. In phase IV, screening potential transporters led to deletion of TAT1 for improving CGA production. Finally, shake-flask fermentation conditions were optimized. The CGA titer significantly increased to 837.2 mg/L in shake-flask cultures and 1.62 g/L in a 5-L bioreactor, respectively.

2. Materials and methods

2.1. Chemicals

The Clon Express II One-Step Kit, Phanta Max Master Mix, and Green Taq Mix DNA polymerase obtained from Vazyme Biotech Co., Ltd. (Nanjing, China). Restriction enzymes, DNA ligase, and DNA gel purification kits were purchased from TaKaRa Bio Inc. (Nanjing, China). The plasmid mini-prep kit and other chemical reagents were purchased from Sangon Biotech Co., Ltd. (Shanghai, China). All codon-optimized heterologous genes (*RgTAL*, *LmXFPK*, and *CkPTA*) and primers were synthesized by Tsingke Biotechnology Co., Ltd. (Beijing, China).

2.2. Strains, Media, and culture conditions

The engineered *S. cerevisiae* strain YC0707 from our previous report was utilized as the host strain in this study [15]. *E. coli* DH5α was used to amplify and construct plasmids. DH5α was cultured at 37 °C and 180 rpm in Luria-Bertain (LB) broth (5 g/L yeast extract, 10 g/L peptone, and 5 g/L NaCl), with 100 μg/mL of kanamycin or ampicillin as needed. The *S. cerevisiae* strains were cultivated at 30 °C and 220 rpm in YPD medium (20 g/L of peptone, 10 g/L of yeast extract, and 20 g/L of glucose).

2.3. Construction of plasmids and strains

All endogenous genes were amplified from *S. cerevisiae* CEN.PK2-1C genomic DNA or from available plasmids. Heterologous genes were amplified using polymerase chain reaction (PCR) with synthesized codon-optimized fragments. The plasmids, codon-optimized genes, and primers used in this study are listed in Tables S1, S2, and S3. For plasmid construction, helper template plasmids were linearized using the restriction enzymes of *Bam*HI, *Xho*I, or *Hin*dIII. The amplified target genes were then assembled into the template plasmids by restricted ligation or Gibson assembly methods to produce gene expression cassettes [27]. The mutants of $PFK2^{S718D}$ and $ARO3^{D154N}$ were constructed by a site-directed mutagenesis system [28]. To construct fusion proteins of adjacent enzymes, a flexible linker, GGGS (GGTGGCGGATCT) [29], was used in this study. Colony polymerase chain reaction was employed to screen for positive clones. The constitutive promoters of *TEF1p*, *PGK1p*, *HXT1p*, and *YEN1p* were amplified from CEN.PK2-1C genomic DNA, including 40bp of upstream and downstream target gene promoter site.

The CRISPR-Cas9 system was employed for gene knockouts and insertions in the genome of *S. cerevisiae* [30]. Guide RNA (gRNA) plasmids targeting genomic spacers were designed by the CHOPCHOP tool (https://chopchop.cbu.uib.no/) [31]. Using plasmid pKan10-ADE2.1 as a template, guide RNA (gRNA) plasmids were constructed by Gibson assembly [32]. All guide target spacers utilized in this study are listed in Table S4. The donor DNA fragments of integration cassettes were amplified from corresponding plasmids, including 40bp of upstream and downstream genomic targets. For gene knockouts, 400 bp upstream and downstream fragments of target genes were amplified and fused by overlap extension PCR [33]. The LiAc/ssDNA/PEG [34] method was employed to co-transform linearized donor fragments (50–100 ng/kb) with corresponding gRNA plasmids (300–500 ng) into *S. cerevisiae*. Transformers were then selected on YPD agar plates containing 200 μg/mL G418. Positive clones were confirmed by colony PCR or Sanger sequencing. All engineering strains used and constructed are listed in Table 1.

2.4. Analysis of RT-qPCR

Transcription levels of *ZWF1*, *GND1*, *PGI1*, and *PFK2* in the engineered strains were quantified by HiScript II® RT SuperMix for qPCR kit from Vazyme Biotech Co., Ltd. (Nanjing, China). Each *S. cerevisiae* strain was cultured in 50 mL of the YPD medium at 30 °C in a shaking incubator (220 rpm) for 36 h. After incubator, 1 mL of the medium was collected and immediately extracted with RNA Plus Reagent. Subsequently, 1 μg of total RNA was reverse-transcribed into cDNA using the HiScript II® RT SuperMix for qPCR kit (Vazyme Biotech, China). The cDNA was then used for further analysis. Quantitative PCR (qPCR) reactions were performed using ChamQTM SYBR® qPCR Master Mix kit (Vazyme Biotech, China) and Bio-Rad CFX Connect Optics Module System (BioRad Laboratories, USA).

2.5. Fermentation conditions

For shake-flask production of CGA, the single colony of engineered *S. cerevisiae* was inoculated into 5 mL of YPD or minimal medium and incubated at 30 °C and 220 rpm for 18–24 h. Subsequently, 2 % of the seed culture was transferred into 250 mL flask containing 50 mL of YPD or minimal medium (25 g/L glucose, 7.5 g/L $(NH4)_2SO_4$, 8 g/L KH_2PO_4, 3 g/L $MgSO_4$, 10 mL/L trace metals solution, and 12 mL/L vitamin solution) [35], maintaining an initial OD_{600} of 0.05. The culture was incubated at 30 °C and 220 rpm for 72 h. Samples were collected every 24 h during shake-flask fermentation.

Fed-batch fermentation was performed in a 5-L bioreactor. The engineered strain YS38 was selected in 5 mL minimal medium at 30 °C and 220 rpm. Next, 2 % of the seed solution was transferred to 250 mL flasks containing 50 mL of minimal medium for 24 h of cultivation. A seed culture of 250 mL was then transferred into the 5-L bioreactor cultivation, with an initial OD_{600} of 0.4. The bioreactor contained 2.0 L of minimal medium (25 g/L glucose, 7.5 g/L $(NH4)_2SO_4$, 8 g/L KH_2PO_4, 3 g/L $MgSO_4$, 10 mL/L trace metals solution, and 12 mL/L vitamin solution). The bioreactor fermentation was performed at 30 °C and 400–800 rpm, with dissolved oxygen levels maintained above 30 %. The pH was controlled at 4.5 by the automatic addition of NH_3H_2O, and the airflow rate was automatically regulated at 2 L/min. When glucose was depleted, the feeding solution (400 g/L glucose, 18 g/L KH_2PO_4, 5 g/L $MgSO_4$, 7 g/L K_2SO_4, 0.56 g/L Na_2SO_4, 10 mL/L trace metals solution, and 12 mL/L vitamin solution) was added to the bioreactor to maintain the glucose concentration below 1.0 g/L. The titers of CGA and OD_{600} were measured through regular sampling during fermentation.

2.6. Analysis method of cell density and the metabolites

Cell density (OD_{600}) was measured using an ultraviolet spectrophotometer.

To determine the concentration of CGA, 500 μL methanol was added to 500 μL of fermentation broth. The mixture was vortexed for 5 min and centrifuged at 12,000 rpm for 10 min. The samples were then filtered through a 0.22 μm organic filter membrane for HPLC analysis. The concentration of CGA was analyzed using an Agilent 1260 HPLC system (Agilent, USA) equipped with a C18 column (250 × 4.6 mm, 5 μm, Agilent, USA) as described previously [15].

A biosensor analyzer SBA-40C (Shandong, China) was utilized to analyze the concentrations of glucose and ethanol.

To analyze the concentration of L-tyrosine, 500 μL of 4 M HCL was added to 500 μL of broth. The mixture was vortexed for 20 min and centrifuged at 12,000 rpm for 10 min. The samples were then filtered through a 0.22 μm organic filter membrane for HPLC assay. The concentration of L-tyrosine was analyzed using an Agilent 1260 HPLC

Table 1
Strains used or constructed in this study.

Strain	Genotype/description	Source
CEN.PK2-1C	*MATa*; *ura3-52*; *trp1-289*; *leu2-3112*; *his3Δ1*; *MAL2-8^{C}*; *SUC2*	Euroscarf
YC0707	CEN.PK2-1C, *X3*::(*GPDp-AtATR1-CYC1t*)-(*ENO2p-CsHQT2-PGK1t*)-(*TPI1p-AtC3′H-TPI1t*)-(*TEF1p-EcYdiB-TEF1t*)-(*PGK1p-At4CL1-HXT7t*)-*HIS3*	Lab stock
YS01	YC0707, *ZWF1p*::*PGK1p*	This study
YS02	YC0707, *ZWF1p*::*TEF1p*	This study
YS03	YS02, *GND1p*::*TEF1p*	This study
YS04	YS03, *TAL1p*::*TEF1p*	This study
YS05	YS04, △*PHO13*	This study
YS06	YS03, *PGI1p*::*YEN1p*	This study
YS07	YS03, *PGI1p*::*HXT1p*	This study
YS08	YS07, *TDH3p*::*HXT1p*	This study
YS09	YS07, *PFK2*::*PFK2^{S718D}*	This study
YS10	YS07, *ENO1p*::*HXT1p*	This study
YS11	YS09, *XIII9*::*TEF1p-LmxFPK-CYC1t*	This study
YS12	YS09, *XIII9*::(*TEF1p-LmxFPK-CYC1t*)-(*PGK1p-CkPTA-HXT7t*)	This study
YS13	YS12, △*GPP1*	This study
YS14	YS09, *X4*::*GPDp-HaTAL-CYC1t*	This study
YS15	YS09, *X4*::*PGK1p-RgTAL-HXT7t*	This study
YS16	YS15, *GAL80*::*PGK1p-ARO3^{D154N}-HXT7t*	This study
YS17	YS15, *IME4p*::*PGK1p*	This study
YS18	YS15, △*RIC1*	This study
YS19	YS15, △*YJL028W*	This study
YS20	YS19, △*HAM1*	This study
YS21	YS20, △*PAD1*	This study
YS22	YS20, △*FDC1*	This study
YS23	YS20, *XIII9*::*PGK1p-RgTAL-(GGGS)-At4CL1-HXT7t*	This study
YS24	YS20, *XIII9*::*GDPp-AtC4H-(GGGS)-At4CL1-HXT7t*	This study
YS25	YS20, *XIII9*::*PGK1p-At4CL1-(GGGS)-CsHQT-PGK1t*	This study
YS26	YS20, *XIII9*::*TEF1p- EcYdiB-(GGGS)-CsHQT-PGK1t*	This study
YS27	YS20, *XIII9*::*ENO2p- CsHQT-(GGGS)-AtC3′H-TPI1t*	This study
YS28	YS24, *X1*::*ENO2p- CsHQT-(GGGS)-AtC3′H-TPI1t*	This study
YS29	YS28, △*OPI1*	This study
YS30	YS28, *INO2p*::*TEF1p*	This study
YS31	YS28, *YJL028W*::*PGK1p-INO2-HXT7t*	This study
YS32	YS31, △*ROX1*	This study
YS33	YS31, △*HMX1*	This study
YS34	YS33, △*ESBP6*	This study
YS35	YS33, △*PDR12*	This study
YS36	YS33, △*ARO80*	This study
YS37	YS33, △*GAL2*	This study
YS38	YS33, △*TAT1*	This study
YS39	YS33, *HMXINO2*::*PGK1p-ESBP6-HXT7t*	This study
YS40	YS33, *HMXINO2*::*TEF1p-PDR12-TEF1t*	This study

system equipped with a C18 column (250 × 4.6 mm, 5 μm, Agilent). The mobile phases consisted of 0.1 M sodium acetate solution (solvent A, pH = 4.0) and 100 % methanol (solvent B). The samples were analyzed for 10 min using the following gradient program: 90 % solvent A for 10 min. The flow rate was 1 mL/min, the injection volume was 10 μL, and the column temperature was maintained at 30 °C. The absorbance of L-tyrosine was detected at 280 nm.

For PEP and E4P analysis, 1 mL of the fermentation broth was sampled at 48 h and immediately quenched with 1 mL of −40 °C methanol. The mixture was centrifuged at 4 °C, 12,000 rpm for 10 min, and the cell pellets were washed by 500 μL of PBS buffer solution. The pellets were then repeatedly frozen in liquid nitrogen and thawed in 37 °C water bath for three times. Following this, the samples were sonicated for 10 min at a power of 300 W, with a cycle of 5 s on and 25 s off. After centrifugation at 4 °C, 12,000 rpm for 5 min, 10 μL of the supernatant was analyzed using PEP and E4P ELISA Kits from Enzyme-linked Biotechnology Co., Ltd. (Shanghai, China).

2.7. Confocal fluorescence microscopy

Yeast cells were cultured in MM medium to maintain strains expressing the HQT-GGGS-C3′H-GFP fusion protein. After cultivating for 48 h at 30 °C with 220 rpm of shaking, cells were washed with HBSS and stained by 1 μM ER-Tracker Blue (Yeasen Biotech, China) at 37 °C for 30 min. Blue fluorescence intensity was monitored with a 374 nm excitation filter and a 474 nm emission filter. Green fluorescence intensity was monitored with a 480 nm excitation filter and a 520 nm emission filter. Then, blue and green fluorescence was observed by fluorescence microscopy (Leica Microsystems CMS GmbH).

3. Results

3.1. Balancing and rewiring carbon distribution of PEP and E4P

PEP and E4P are directly connected the central carbon metabolism to the CGA synthetic pathway [36]. Given that the concentration of PEP is at least one order of magnitude higher than that of E4P in *S. cerevisiae* [37], we sought to balance the carbon distribution between PEP and E4P by enhancing the PPP pathway and attenuating the EMP pathway (Fig. 2A). ZWF1 (glucose-6-phosphate 1-dehydrogenase) and GND1 (6-phosphogluconate dehydrogenase) within the PPP pathway are crucial for supplying E4P and regenerating NADPH in *S. cerevisiae* [38]. The constitutive strong promoters of P_{PGK1} and P_{TEF1} are extensively studied and applied in *S. cerevisiae* [39]. Therefore, we enhanced the expression of *ZWF1* by replacing its original promoter with two reported strong promoters P_{PGK1} and P_{TEF1} in YC0707. The relative transcription level of *ZWF1* was significantly increased by promoter P_{TEF1} and P_{PGK1}, while P_{TEF1} is better than P_{PGK1}. The relative transcription level of *ZWF1* in strain YS02 was 74.2 % higher in strain YS02 than that in YS01 strain (Fig. S2). This increased CGA production, reaching 272.8 mg/L and

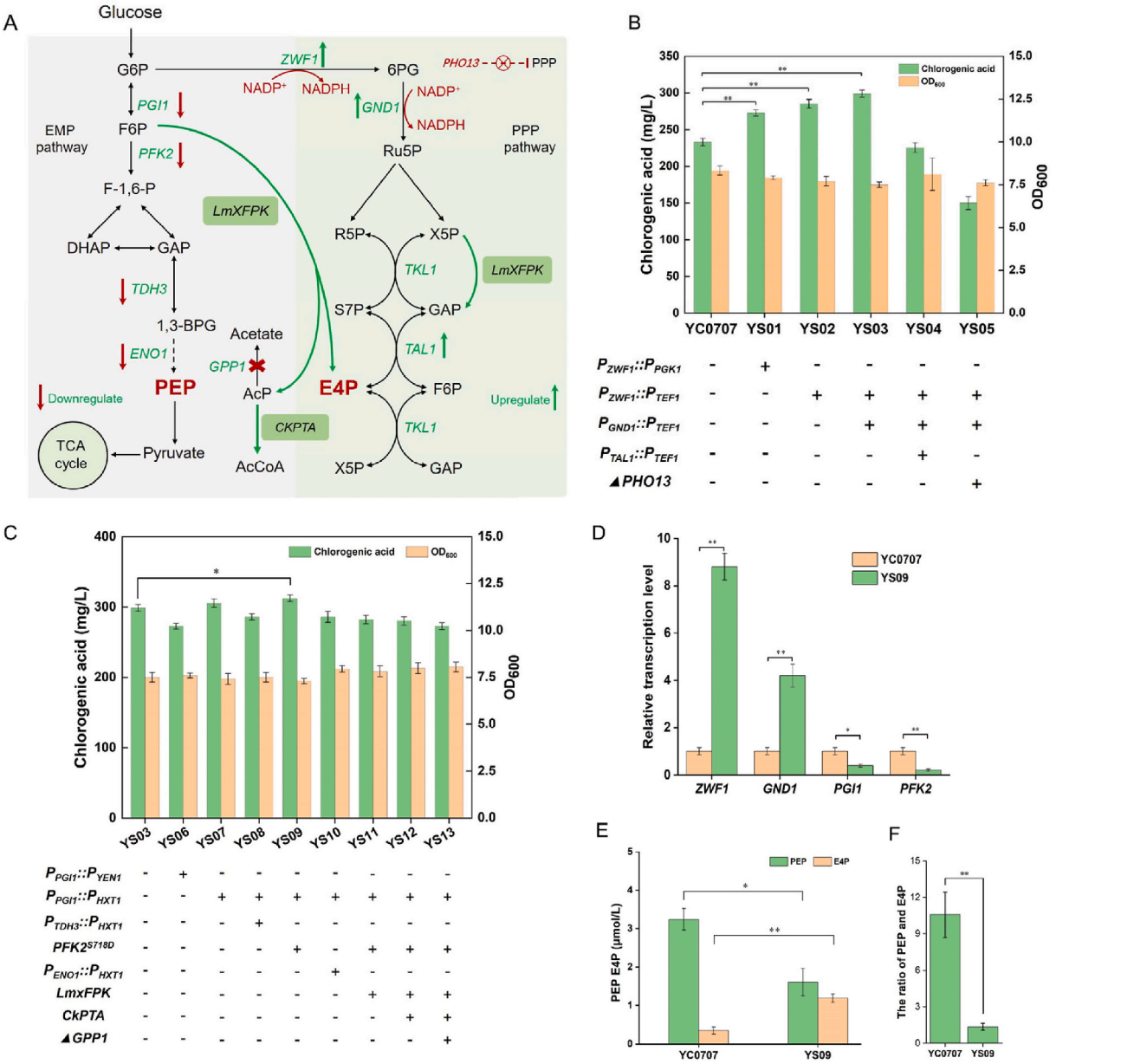

Fig. 2. Increasing CGA production by balancing E4P and PEP supply. **(A)** Metabolic engineering strategy for balancing the supply of E4P and PEP, including strengthening PPP pathway and restricting EMP pathway. X5P: D-xylulose 5-phosphate; R5P: D-ribose 5-phosphate; F6P: beta-D-fructose 6-phosphate; GAP: glyceraldehyde 3-phosphate. ZWF1, glucose-6-phosphate dehydrogenase; GND1, 6-phosphogluconate dehydrogenase; TAL, transaldolase; PGI1, phosphoglucose isomerase; PFK2^{S718D}, phosphofructokinase mutant; TDH3, glyceraldehyde-3-phosphate dehydrogenase; ENO1, phosphopyruvate hydratase; GPP1, GAP phosphatase; LmXFPK, phosphoketolase; CkPTA, phosphotransferase. **(B)** CGA production and OD_{600} after upregulation of the *ZWF1*, *GND1*, and *TAL1* genes and deleting *PHO13* in PPP pathway. **(C)** CGA production and OD_{600} after downregulation of the *PGI1*, *TDH3*, *PFK2*, and *ENO1* genes in EMP pathway and introducing PHK pathway genes. **(D)** The relative transcription levels of *ZWF1*, *GND1*, *PGI1*, and *PFK2* in engineered strain YC0707 and YS09 for cultivating 48h. **(E)** The concentrations of PEP and E4P in engineered strain YC0707 and YS09 for cultivating 48h. **(F)** The ratio of PEP and E4P in strain YC0707 and YS09. Engineered strains for producing CGA were cultivated in minimal medium with 25 g/L glucose for 72h. The displayed average values and standard deviations were calculated from three biological replicates (*$P < 0.05$, **$P < 0.01$).

285.2 mg/L of CGA in YS01 and YS02 (Fig. 2B). These CGA titers represented significant improvements of 16.2 % and 21.5 % compared to YC0707. The *GND1* promoter was then replaced by P_{TEF1} in YS02, resulting in strain YS03, which further increased CGA production to 298.8 mg/L (Fig. 2B). As expected, the relative transcription levels of *ZWF1* and *GND1* increased by 8.8-fold and 4.2-fold compared to the parent strain YC0707 (Fig. 2D). Given that transaldolase (TAL) catalyzes the conversion of sedoheptulose-7-phosphate (S7P) and glyceraldehyde 3-phosphate (GAP) to erythrose 4-phosphate (E4P) and fructose 6-phosphate (F6P) [40], we replaced its original promoter with the strong promoter P_{TEF1} in YS03. However, the CGA titer decreased to 225.4 mg/L in resultant strain YS04 (Fig. 2B). *PHO13* exhibits specific dephosphorylating activity on 4-phosphoerythronate, and deletion of *PHO13* upregulates the transcription of genes involved in the PPP pathway [41]. Nevertheless, there was a 48.9 % decrease in CGA titer to 152.6 mg/L when *PHO13* was deleted in YS03 (Fig. 2B).

To weaken the carbon flux through the EMP pathway in *S. cerevisiae*, several key enzyme genes were selected to downregulate their expressions [42]. *PGI1* encodes phosphoglucose isomerase, and we replaced its original promoter with the weak promoters P_{YEN1} and P_{HXT1} in strain

YS03. However, the resultant strain YS06 and YS07 exhibited CGA titers of 272.1 mg/L and 305.2 mg/L (Fig. 2C). *PFK2* (encoding phosphofructokinase) is the rate-limiting enzyme of the EMP pathway, the mutant gene of $PFK2^{S718D}$ has been demonstrated to decrease the conversion from fructose-6-phosphate (F6P) to fructose-1,6-diphosphate (F-1,6-P) [43]. $PFK2^{S718D}$ was then introduced into the strain YS07, CGA titers increased to 314.4 mg/L in resultant strain YS09 (Fig. 2C). The original promoters of *TDH3* (encoding glyceraldehyde-3-phosphate dehydrogenase) and *ENO1* (encoding phosphopyruvate hydratase) were then replaced with the weak promoter P_{HXT1} in strain YS07, the resultant strain YS08 and YS10 decreased CGA titers of 285.8 mg/L and 277.8 mg/L, respectively. Overall, the titer of CGA increased from 298.8 mg/L to 314.4 mg/L by replacing P_{PGI1} with P_{HXT1} and introducing $PFK2^{S718D}$. The relative transcription levels of *PGI1* and *PFK2* in YS09 decreased by 60 % and 80 % compared to the parent strain YC0707 (Fig. 2D). In strain YS09, the concentration of PEP decreased by 1.3-fold, while the concentration of E4P increased by 3.2-fold compared to YC0707 (Fig. 2E). Additionally, the ratio of PEP and E4P decreased from 10.58 to 1.35, efficiently balancing the supply of PEP and E4P in YS09 (Fig. 2F).

The heterogeneous phosphoketolase (PHK) pathway, consisting of phosphoketolase (FPK) and phosphotransacetylase (PTA), could catalyze the conversion of F6P to E4P [44]. PHK pathway was introduced by integrating *XFPK* from *Leuconostoc mesenteroides* and *PTA* from *Clostridium kluyveri* into the genomic locus of *GPP1* to enhance E4P supply on the base strain YS09. Unexpectedly, the titer of CGA decreased to 270.8 mg/L in resultant strain YS13 (Fig. 2C).

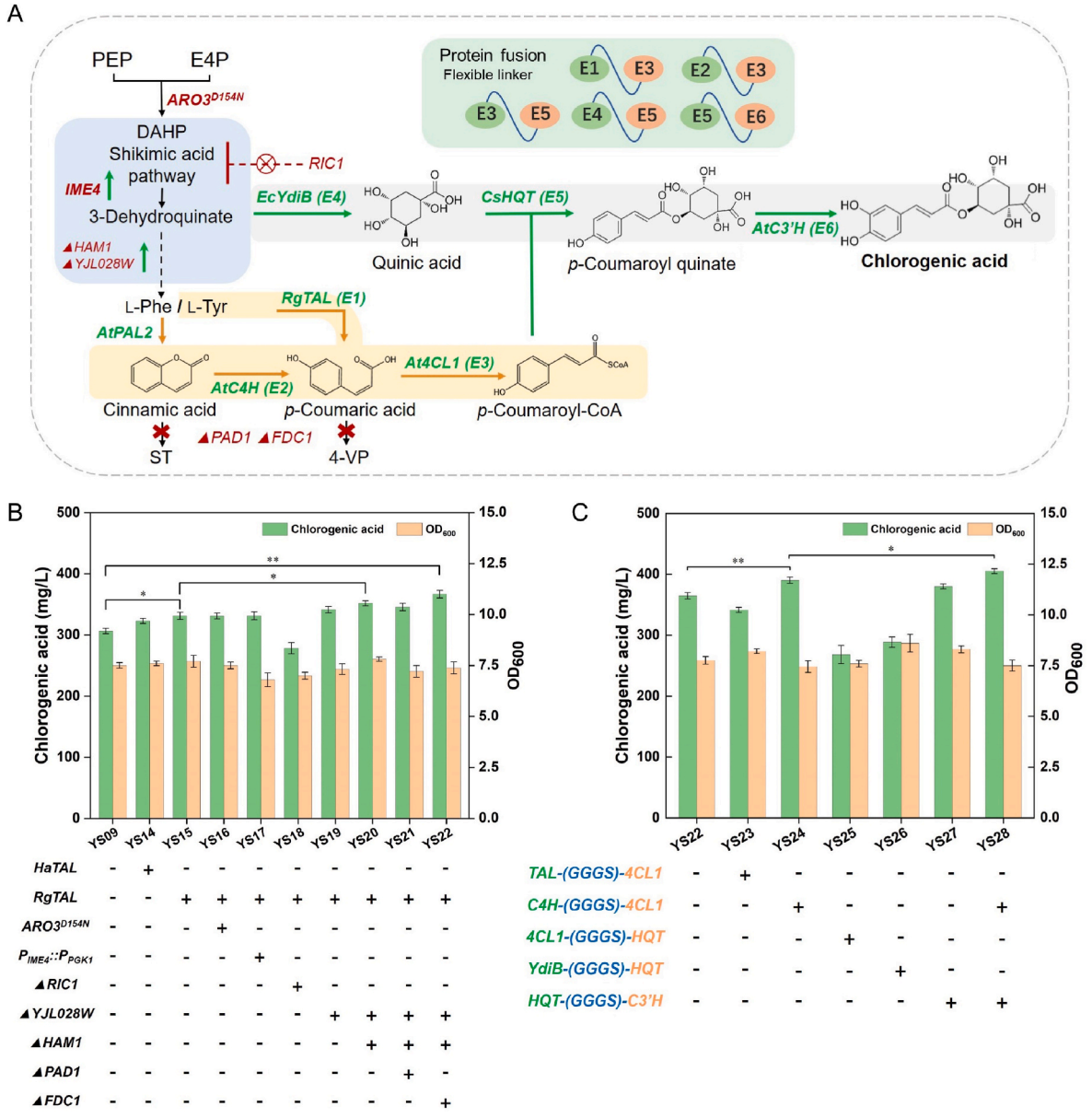

Fig. 3. Optimization of *p*-coumaric acid pathway and fusion enzyme strategy increase CGA production. DAHP: 3-deoxy-D-arabino-heptulosonate-7-phosphate; L-Phe: L-phenylalanine; L-Tyr: L-tyrosine; ST: styrene; 4-VP: 4-vinylphenol; FDC1: ferulic acid decarboxylase; PAD1: phenylacrylic acid decarboxylase. HAM1, nucleoside triphosphate pyrophosphohydrolase. YJL028W, a protein of unknown function that might interact with ribosomes. **(A)** Strategy for enhancing *p*-coumaric acid pathway and fusion enzyme strategy for CGA production. The adjacent enzymes of RgTAL (E1), AtC4H (E2), At4CL1 (E3), EcYdiB (E4), CsHQT (E5), and AtC3′H (E6) were fused by flexible linker (GGGS). **(B)** Effects of enhancing the aromatic acids pathway on the titer of CGA. **(C)** CGA production after fusion expression of different adjacent enzymes. Engineered strains were cultivated in minimal medium with 25 g/L glucose for 72 h. Cultures were sampled at the end of fermentation. The displayed average values and standard deviations were calculated from three biological replicates ($*P < 0.05$, $**P < 0.01$).

3.2. Optimization of p-coumaric acid pathway and substrate trafficking engineering enhance CGA biosynthesis

The supply of *p*-coumaric acid is a key precursor for CGA synthesis. It has been reported that synergizing both the L-tyrosine branch and L-phenylalanine branches is more effective than relying solely on the L-phenylalanine branch [37]. Tyrosine ammonia lyase from *Herpetosiphon aurantiacus* (HaTAL) showed higher titer in resveratrol synthesis than other resource TAL such as FjTAL from *Flavobacterium johnsoniaeu* [45]. RgTAL from *Rhodotorula glutinis* also showed better tyrosine specificity than other TALs [46]. Thus, HaTAL and RgTAL was selected to enhance the conversion from L-tyrosine to *p*-coumaric acid. The resulting strain YS14, which integrated *HaTAL*, produced 322.8 mg/L of CGA, with the L-tyrosine titer decreasing from 252.8 mg/L to 165.4 mg/L. The resultant strain YS15, which integrated *RgTAL*, produced 334.2 mg/L of CGA (Fig. 3B), with the L-tyrosine titer decreasing to 135.2 mg/L (Fig. S1). These results indicate that *RgTAL* is more efficient in converting L-tyrosine to *p*-coumaric acid for CGA synthesis. Additionally, it has been reported that the DAHP synthase mutant of $ARO3^{D154N}$ could relieve the feedback inhibition by phenylalanine [47]. The resultant strain YS16 reached a CGA titer of 330.8 mg/L by introducing $ARO3^{D154N}$ into strain YS15. The transcript levels of ARO1 (pentafunctional aromatic protein) and ARO2 (chorismate synthase) can be upregulated by overexpressing IME4 (an mRNA N6-adenosine methyltransferase) [48]. Here, the promoter of *IME4* was replaced by strong promoter P_{PGK1} in strain YS16, resulting in a CGA titer of 331.2 mg/L (YS17) without improvement (Fig. 3B). Previous studies have discovered that the deletion of *RIC1*, *YJL028W*, and *HAM1* significantly improves the synthesis efficiency of aromatic acids [10,49]. Consequently, we deleted these genes in strain YS16, resulting in strains YS18, YS19, and YS20, which produced 278.8 mg/L, 341.1 mg/L, and 352.8 mg/L of CGA, respectively (Fig. 3B). Endogenous enzymes PAD1 (phenylacrylic acid decarboxylase) and FDC1 (ferulic acid decarboxylase) are involved in the decarboxylation of phenylacrylic acids [50]. To eliminate the decarboxylation pathways of coumaric acids, *PAD1* and *FDC1* were deleted in strain YS20, resulting in strains YS21 and YS22, which reached CGA titers of 345.6 mg/L and 362.7 mg/L, respectively (Fig. 3B). This result showed that removal of *FDC1* facilitated the production of CGA. Overall, the titer of CGA represented a 17.9 % improvement by optimization of aromatic compounds pathway.

The substrate diffusion effect may reduce the reaction efficiency from 3-dehydroquinate and *p*-coumaric acid to CGA [51]. To address this, fusion expression between enzymes using peptide linkers can speeding up the turnover of intermediates and improving reaction flux [52]. The flexible linker GGGS was more suitable for the fusion expression and synthesis of *p*-coumaric acid derivatives, such as isoflavonoids and naringenin [53,54]. Therefore, the flexible linker GGGS was used to fuse adjacent enzyme sequences. Specifically, we fused RgTAL-linker-At4CL1 (E1-E3), AtC4H-linker-At4CL1 (E2-E3), At4CL1-linker-CsHQT (E3-E5), EcYdiB-linker-CsHQT (E4-E5), and CsHQT-linker-AtC3′H (E5-E6), which were introduced into strain YS22 (Fig. 3A). As shown in Fig. 3C, the CGA titers of the resultant strains YS23–YS27 were 341.4 mg/L (E1-E3), 390.2 mg/L (E2-E3), 268.2 mg/L (E3-E5), 289.5 mg/L (E4-E5), and 379.9 mg/L (E5-E6), respectively. The fusion expressions of AtC4H-linker-At4CL1 and CsHQT-linker-AtC3′H led to the creation of strain YS28, which produced 405.2 mg/L of CGA, representing an 12.2 % increase compared with the parent strain YS22. A confocal microscopy analysis of yeast cells (Fig. S4) showed that the HQT-(GGGS)-C3′H fusion protein mainly localized in the yeast cytoplasm, and a small amount localized to the ER.

3.3. Improving the microenvironment of P450s for CGA production

Cytochrome P450 enzymes involved in the biosynthesis of plant-specialized products are considered as rate-limiting steps in *S. cerevisiae* [55]. Therefore, we focused on improving the microenvironment of P450s for CGA production. Most cytochrome P450 reductases are membrane-bound proteins localized to the endoplasmic reticulum (ER) [56]. The key ER regulatory factors, *OPI1* and *INO2*, are responsible for regulating phospholipid synthesis [57]. Firstly, we deleted *OPI1* in strain YS28 to create strain YS29, which decreased CGA titer to 372.8 mg/L (Fig. 4B). Subsequently, we overexpressed *INO2* by replacing its original promoter with strong promoter P_{TEF1} and by introducing an additional *PGK1p-INO2-HXT7t* cassette into strain YS28. The resultant strains YS30 and YS31 increased CGA titers to 414.2 mg/L and 425.1 mg/L, respectively (Fig. 4B). In addition to ER expansion, the formation of active P450s requires more supply of cofactor heme [58]. The heme-dependent transcriptional repressor *ROX1* inhibits the heme biosynthetic gene *HEM13*, and *HMX1* involved in heme oxygenase [59,60]. Accordingly, we deleted *ROX1* and *HMX1* to promote heme metabolism in strain YS31. The resulting strains YS32 and YS33 reached CGA titers of 392.5 mg/L and 440.9 mg/L, respectively (Fig. 4B). These results showed that overexpressing *INO2* and deleting *HMX1* led to a 10.1 % improvement in CGA titers compared to strain YS28.

3.4. Screening potential transporters for CGA production

Transporter engineering is essential for accumulating extracellular products. Transporters (*ESBP6* and *PDR12*) can increase tolerance to aromatic acids at low pH, and *ARO80* activates transcription of aromatic acids synthetic genes in the presence of aromatic amino acids [61]. Therefore, deletions of *ESBP6*, *PDR12*, and *ARO80* were performed in the base strain YS33, causing resulted strains of YS34, YS35, and YS36, which produced CGA titers of 408.8 mg/L, 425.2 mg/L, and 390.2 mg/L, respectively (Fig. 5B). Meanwhile, we enhanced the expression of *ESBP6* and *PDR12* by introducing additional *PGK1p-ESBP6-HXT7t* cassette and *TEF1p-PDR12-TEF1t* cassette in strain YS33. The titer of CGA in resulting strains YS39 and YS40 decreased to 345.6 mg/L and 368.7 mg/L (Fig. 5B). Furthermore, two transporters (TAT1 and GAL2) involved in the transport of L-tyrosine and galactose [62]. Consequently, we deleted *GAL2* and *TAT1* in strain YS33, and the resultant strains YS37 and YS38 produced 339.1 mg/L and 459.8 mg/L of CGA, respectively (Fig. 5B). Overall, we achieved a slight increase in CGA titers by knocking out the transporter of TAT1.

3.5. Fermentation optimization for CGA production

Stable and optimal culture conditions are critical for the synthesis of target products [63]. To optimize shake-flask culture conditions for CGA production, the best-performing strain YS38 was selected for fermentation optimization, as it produced 459.8 mg/L of CGA in the minimal medium and 309.6 mg/L in the YPD medium (Fig. 6A). Firstly, we investigated the effects of different carbon and nitrogen sources on CGA production. Different carbon sources, such as glucose, sucrose, fructose, and starch were tested for fermentation, resulting in CGA titers of 456.8 mg/L, 320.8 mg/L, 275.4 mg/L, and 95.9 mg/L in shake-flask cultures (Fig. 6B). These results showed glucose was the best carbon source for CGA production. Subsequently, different nitrogen sources of ammonium sulfate, ammonium chloride, ammonium ferric citrate, beef extract, yeast extract, and peptone were evaluated in shake-flask culture. The yield of CGA was higher than that of other nitrogen sources when utilizing ammonium sulfate as a nitrogen source (Fig. 6C). Then, strain YS38 was cultured at different initial pH levels (4.0, 4.5, 5.0, 5.5, and 6.0), with the highest CGA titer of 458.2 mg/L at pH 4.5 (Fig. 6D). There are little bioproducts of *p*-coumaric acid and caffeic acid in shaking-flask fermentation process, all less than 15 mg/L (Fig. S3). We further investigated different glucose concentrations of 25 g/L, 50 g/L, 75 g/L, and 100 g/L in shake-flask cultures, yielding CGA titers of 458.4 mg/L, 669.1 mg/L, 837.2 mg/L, and 897.6 mg/L, respectively (Fig. 6E). The optimized shake-flask culture conditions, including minimal medium with 75 g/L glucose and an initial pH level of 4.5, resulted in an 82.1 % improvement of CGA titers, from 459.8 mg/L to 837.2 mg/L (Fig. 6F).

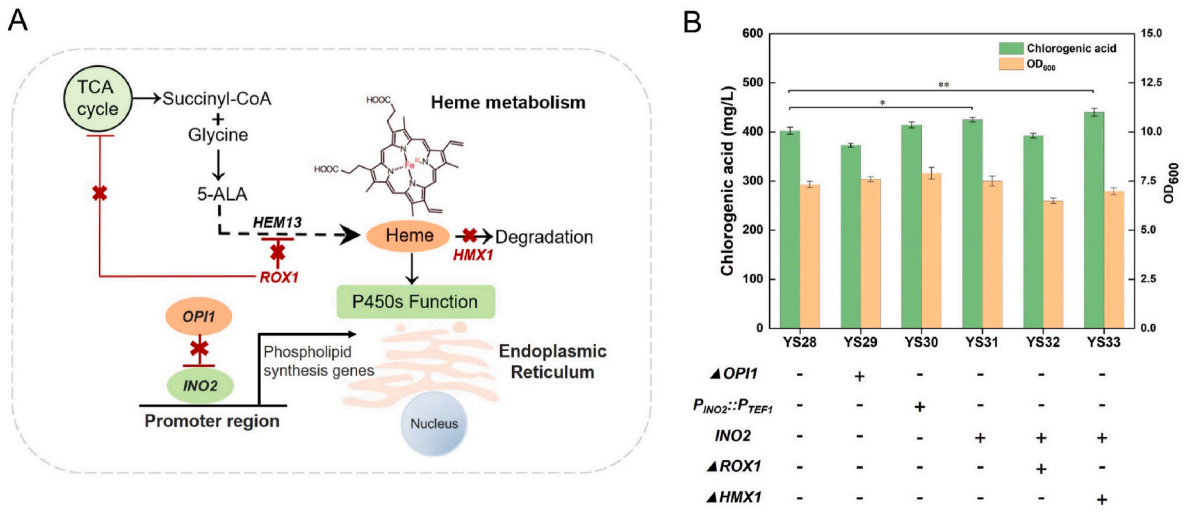

Fig. 4. Improving the microenvironment of P450 enzymes for CGA production.
HEM13, coproporphyrinogen III oxidase gene; *HMX1*, heme oxygenase gene; *ROX1*, heme-dependent repressor of hypoxic genes; *INO2*, a transcription factor for lipid biosynthesis; *OPI1*: the transcriptional repressor of *INO2*. **(A)** Strategies for ER engineering and heme supply to improve the microenvironment of P450s. **(B)** Effects of engineering the endoplasmic reticulum (ER) size and increasing heme supply on CGA titer. Engineered strains were cultivated in minimal medium with 25 g/L glucose for 72 h. Cultures were sampled at the end of fermentation. The displayed average values and standard deviations were calculated from three biological replicates (*$P < 0.05$, **$P < 0.01$).

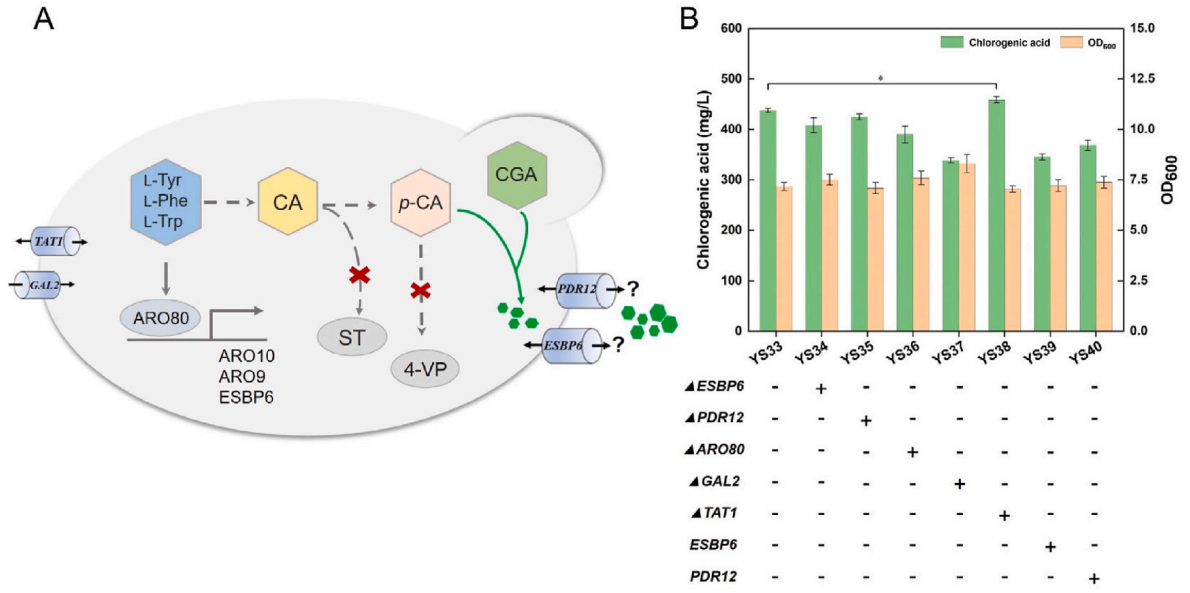

Fig. 5. Screening transporters for CGA production. L-Trp: L-tryptophan; L-Phe: L-phenylalanine; L-Tyr: L-tyrosine; CA: cinnamic acid; *p*-CA: *p*-coumaric acid. ESBP6, protein with similarity to monocarboxylate permeases; TAT1, tyrosine and tryptophan amino acid transporter; GAL2, galactose permease; PDR12 and ESBP6, two transporters of increasing tolerance to aromatic acids. **(A)** The transporters of aromatic acids and coumaric acids in *S. cerevisiae*. **(B)** Effects of deleting transporters and introducing additional copy of transporters on CGA production. Engineered strains were cultivated in minimal medium with 25 g/L glucose for 72 h. Cultures were sampled at the end of fermentation. The displayed average values and standard deviations were calculated from three biological replicates (*$P < 0.05$, **$P < 0.01$).

The engineered strain YS38 was selected for fed-batch fermentation in a 5-L bioreactor with an initial volume of 2 L of the minimal medium same to the optimized shake-flask culture medium. However, when the initial glucose concentration was 75 g/L, the accumulation of ethanol in 5-L bioreactor was serious, and the glucose was completely consumed until 48 h. As shown in Fig. S6A, the growth of yeast was inhibited by high concentration of ethanol (30 g/L) during the fed-batch fermentation process. CGA titers reached 0.92 g/L, 1.29 g/L, and 1.62 g/L with initial glucose concentrations of 75 g/L, 50 g/L, and 25 g/L, respectively. The synthetic efficiency of CGA was the highest in 5-L bioreactor when initial glucose concentration was 25 g/L. As illustrated in Fig. 7, the OD_{600} reached a maximum of 41.2 after 60 h of fermentation, and the CGA titer reached 1.62 g/L after 60 h. To the best of our knowledge, this titer represents the highest yield of CGA in *S. cerevisiae*.

4. Discussion

Chlorogenic acid (CGA), a phenolic acid compound, exhibits diverse pharmaceutical properties [64]. In this study, we employed a systematic metabolic engineering strategy through chromosomal modification to construct high-performing strain for CGA production. The titer of CGA increased from 234.8 mg/L to 837.2 mg/L in shake flasks through

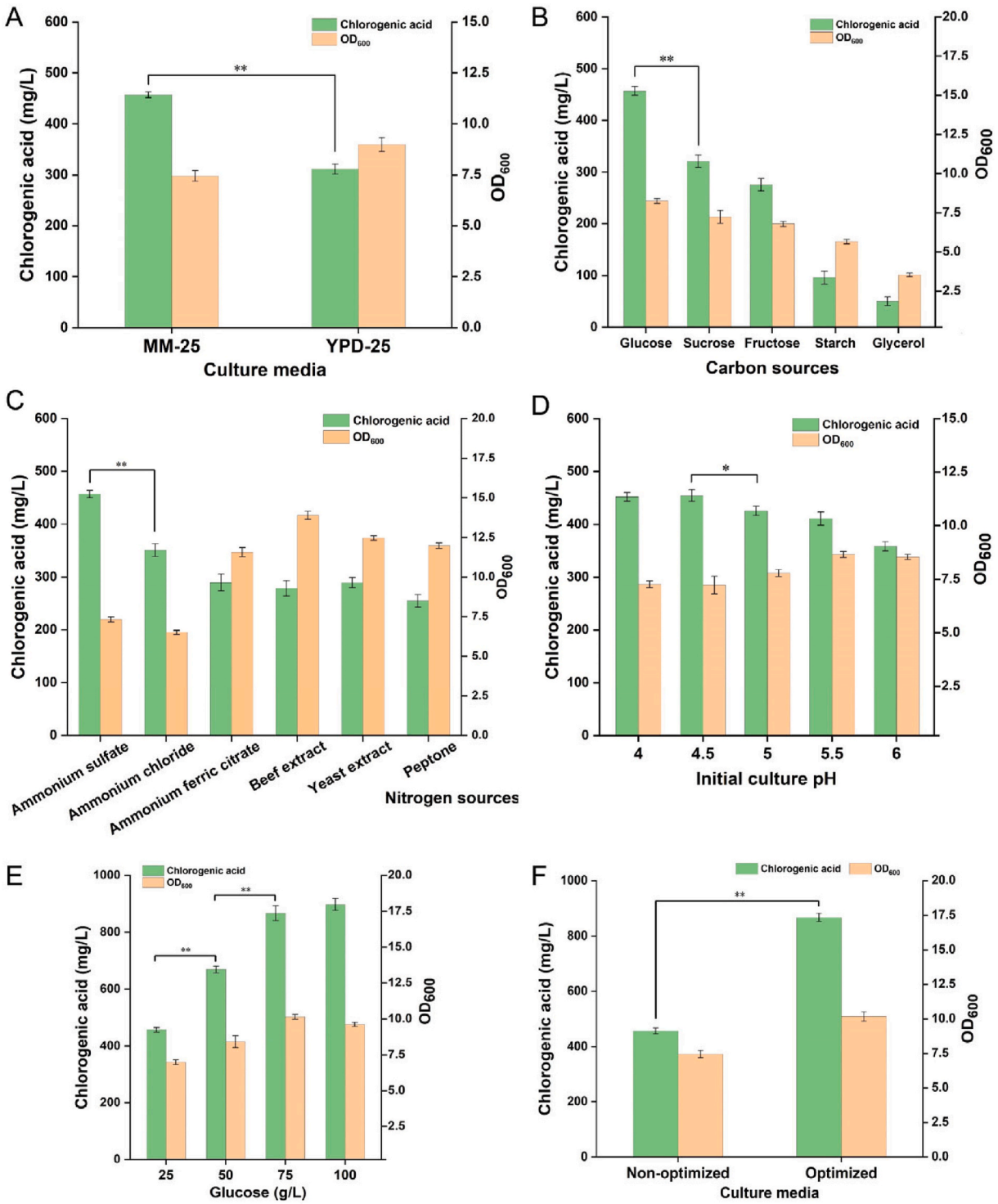

Fig. 6. Shake-flask fermentation optimization for CGA production. **(A)** CGA production of engineered strain YS38 in minimal medium and YPD medium with 25 g/L glucose. **(B)** Effects of different carbon sources on CGA production in minimal medium with 25 g/L glucose. **(C)** Effects of different nitrogen sources on CGA production in minimal medium with 25 g/L glucose. **(D)** Effects of different pH on CGA production in minimal medium with 25 g/L glucose. **(E)** Effects of different glucose concentrations on CGA production in minimal medium. **(F)** The yield of CGA in non-optimized culture and optimized culture. Cultures were sampled at the end of fermentation. The displayed average values and standard deviations were calculated from three biological replicates (*$P < 0.05$, **$P < 0.01$).

balancing carbon distribution of PEP and E4P, optimizing *p*-coumaric acid pathway, fusion expression of key enzymes, improving the micro-environment of P450s, screening potential transporters, and optimizing fermentation conditions.

In previous studies, different strategies have been used to improve CGA production in engineered *E. coli* and *S. cerevisiae* [14,15], however, fewer studies focused on balancing the carbon distribution of PEP and E4P for aromatic compounds production. In this study, the expression of PPP pathway genes was upregulated by replacing the original promoters of *ZWF1* and *GND1* with strong promoter P_{TEF1}. Since P_{TEF1} exhibited more stable and higher activity compared with P_{PGK1}, this result is consistent with the previous literature [65]. The expression of EMP

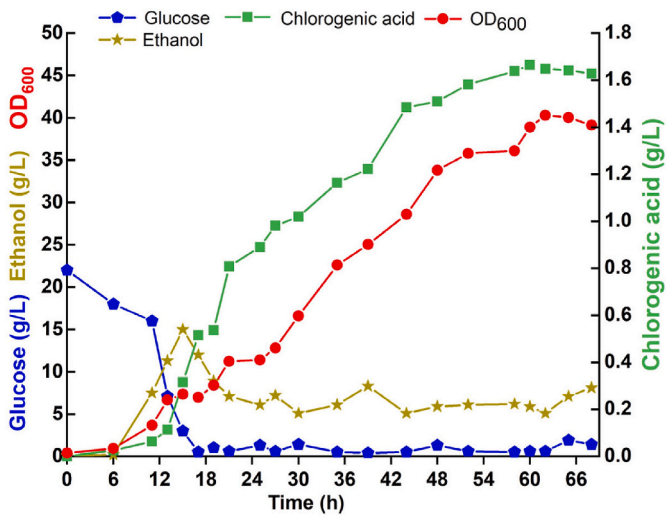

Fig. 7. The CGA production of YS38 in a 5-L bioreactor by fed-batch strategy.

pathway genes was downregulated by replacing the native promoter of *PGI1* with weak promoter P_{HXT1} and introducing the mutant of $PFK2^{S718D}$. This strategy adjusted the ratio of PEP and E4P from 10.58 to 1.35 in engineered strain YS09 (Fig. 2F), which indicated that the balance of PEP and E4P was beneficial for CGA production. However, the decreased supply of PEP resulted in the worse cell growth in shake flasks, the OD_{600} of engineered strain reduced from 8.5 (YC0707) to 6.7 (YS09). In order to balance CGA production and cell growth in engineered strain, the optimal ratio of PEP and E4P for CGA synthesis remains to be investigated in the future. Meanwhile, the heterogeneous PHK pathway significantly decreased CGA titers (Fig. 2C), probably due to LmXFPK not only catalyzed F6P to E4P but also exhibited high activity in converting X5P to GAP [66]. The decrease in CGA titers may be associated with a low intracellular concentration of F6P.

The *p*-coumaric acid biosynthetic pathway is the bottleneck for CGA biosynthesis [37]. In this study, the conversion from L-tyrosine to *p*-coumaric acid was firstly increased by introducing RgTAL. Then, the metabolic flux from DAHP to p-coumaric acid was increased by knocking out *YJL028W*, *HAM1*, and *FDC1*. Fusion expression of neighbor-reaction-step enzymes, including the P450 enzymes AtC4H and AtC3′H, may enhance CGA production. Among all the fusion strategies in this study, the combination of C4H-GGGS-4CL1 and HQT-GGGS-C3′H improved the synthesis of CGA, suggesting that the suitable combination of neighbor-reaction-step enzymes is crucial for enhanced CGA production. Confocal microscopy analysis showed HQT-(GGGS)-C3′H mainly localized in the cytoplasm, and a small amount localized to the ER (Fig. S4). However, ER localization of P450s may not be the optimal strategy for CGA production, too many P450s localized to the ER may result in ER crowding and potentially affecting other necessary proteins synthesis on ribosomes. Moreover, only partial enzymes in the pathway of CGA synthesis were fused [37,51]. Therefore, more enzymes and ER-localization of P450s, still require to be evaluated for their effect on CGA production.

Expanding the endoplasmic reticulum (ER) and improving cofactor heme biosynthesis can improve the catalytic microenvironment of P450s [25,67]. In this study, the expression of the key ER regulatory factor *INO2* was enhanced to improve the ER homeostasis, which resulted in a significant improvement in CGA titer (Fig. 4B). The enhanced CGA titers may cause by the abundance increasing of ER-related P450s. However, it is not clear how ER expansion promotes P450s synthesis [57]. Furthermore, heme oxygenase gene *HMX1* and heme-dependent repressor of hypoxic gene *ROX1* was deleted to enhance heme biosynthetic metabolism. The result showed that only the deletion of *HMX1* facilitated CGA accumulation, while the removal of *ROX1* decreased CGA production and final cell growth (Fig. 4B), likely due to the loss of its regulatory role in *S. cerevisiae* stress resistance [25]. Overall, we only improved the microenvironment of P450s through existing reports, it is not certain that these P450s have been fully expressed and localized to the ER. In the future, the effect of combining the P450s, such as C3′H and C4H, with ER on CGA production require to be evaluated.

Transporter engineering can alleviate metabolic pressure on cells and enhance production of target products [68]. Transporters of *ESBP6* and *PDR12* found to be related to the tolerance of aromatic acids at low pH [61], we respectively knocked out and overexpressed them to examine their effects on CGA production. However, neither of these transporters contributed to an increase in CGA yield, indicating these transporters are not directly involved in CGA efflux, or that they may have potential isoenzymes with similar functions. This is consistent with the main distribution of CGA in extracellular (Fig. S5). Moreover, knockout of tyrosine transporter gene *TAT1* led to the improvement of CGA titer (Fig. 5B), this potentially being caused by the decreased leakage of intracellular tyrosine [62]. More efforts should focus on reducing the loss of precursors and maintaining the appropriate concentration of precursors in the cell by transport engineering.

In summary, a system metabolic engineering strategy resulted in CGA titers to 837.2 mg/L in shake flasks, and 1.62 g/L in a 5-L bioreactor, respectively. We found high initial glucose concentration was not suitable for CGA production in fed-batch fermentation, which is not consistent with the result of initial glucose concentration of 75 g/L in shake flasks. Because the accumulation of ethanol was more serious and the initial glucose was completely consumed until 48 h in 5-L bioreactor (Fig. S6). The synthetic efficiency of CGA was highest during fed-batch fermentation when initial glucose concentration was 25 g/L. This study significantly improves CGA productivity and provides valuable insights into the biosynthesis of CGA derivatives. Compared to the previous publications on engineered *E. coli* and yeast for CGA production [14,15], the CGA titer in shake flasks in this study is higher than that in other studies. However, the CGA titers and final cell density in 5-L bioreactor were limited (Fig. 7). It may result from the decrease of the EMP pathway carbon flux to the TCA cycle, which resulted in the decrease of cell growth. Future studies should focus on optimizing the balance between cell growth and CGA production.

CRediT authorship contribution statement

Shuai Tu: Writing – original draft, Visualization, Project administration, Methodology, Investigation. **Junjie Wang:** Methodology, Investigation. **Pengming Yang:** Methodology, Investigation. **Yan He:** Visualization, Methodology, Investigation. **Zhixing Gong:** Visualization, Methodology. **Weihong Zhong:** Writing – review & editing, Supervision, Project administration, Funding acquisition, Conceptualization.

Declaration of competing interest

The authors declare that they have no known competing financial interests or personal relationships that could have appeared to influence the work reported in this paper.

Acknowledgments

This work was partially financially supported by National Key Research and Development Program of China (2021YFA0909500) and the National Natural Science Foundation of China (no.31970104).

Appendix A. Supplementary data

Supplementary data to this article can be found online at https://doi.org/10.1016/j.synbio.2025.03.004.

References

[1] Upadhyay R, Mohan Rao LJ. An outlook on chlorogenic acids—occurrence, chemistry, technology, and biological activities. Crit Rev Food Sci Nutr 2013;53:968–84. https://doi.org/10.1080/10408398.2011.576319.

[2] Bhandarkar NS, Brown L, Panchal SK. Chlorogenic acid attenuates high-carbohydrate, high-fat diet–induced cardiovascular, liver, and metabolic changes in rats. Nutr Res 2019;62:78–88. https://doi.org/10.1016/j.nutres.2018.11.002.

[3] Lukitasari M, Nugroho DA, Widodo N. Chlorogenic acid: the conceivable chemosensitizer leading to cancer growth suppression. J Evid Based Integr Med 2018;23:2515690X1878962. https://doi.org/10.1177/2515690X18789628.

[4] Sun Z, Zhang X, Wu H, Wang H, Bian H, Zhu Y, et al. Antibacterial activity and action mode of chlorogenic acid against *Salmonella* Enteritidis, a foodborne pathogen in chilled fresh chicken. World J Microbiol Biotechnol 2020;36:24. https://doi.org/10.1007/s11274-020-2799-2.

[5] Wang L, Pan X, Jiang L, Chu Y, Gao S, Jiang X, et al. The biological activity mechanism of chlorogenic acid and its applications in food industry: a review. Front Nutr 2022;9:1–22. https://doi.org/10.3389/fnut.2022.943911.

[6] Santana-Gálvez J, Cisneros-Zevallos L, Jacobo-Velázquez D. Chlorogenic acid: recent advances on its dual role as a food additive and a nutraceutical against metabolic syndrome. Molecules 2017;22:358. https://doi.org/10.3390/molecules22030358.

[7] Niggeweg R, Michael AJ, Martin C. Engineering plants with increased levels of the antioxidant chlorogenic acid. Nat Biotechnol 2004;22:746–54. https://doi.org/10.1038/nbt966.

[8] Li Y, Kong D, Bai M, He H, Wang H, Wu H. Correlation of the temporal and spatial expression patterns of HQT with the biosynthesis and accumulation of chlorogenic acid in *Lonicera japonica* flowers. Hortic Res 2019;6:73. https://doi.org/10.1038/s41438-019-0154-2.

[9] Xiong D, Lu S, Wu J, Liang C, Wang W, Wang W, et al. Improving key enzyme activity in phenylpropanoid pathway with a designed biosensor. Metab Eng 2017;40:115–23. https://doi.org/10.1016/j.ymben.2017.01.006.

[10] Jia Z-C, Liu D, Ma H-D, Cui Y-H, Li H-M, Li X, et al. Yeast metabolic engineering for biosynthesis of caffeic acid-derived phenethyl ester and phenethyl amide. ACS Synth Biol 2023;12:3635–45. https://doi.org/10.1021/acssynbio.3c00413.

[11] Kim BG, Jung WD, Mok H, Ahn JH. Production of hydroxycinnamoyl-shikimates and chlorogenic acid in *Escherichia coli*: production of hydroxycinnamic acid conjugates. Microb Cell Fact 2013;12:1–11. https://doi.org/10.1186/1475-2859-12-15.

[12] Niu FX, Yan ZB, Huang Y Bin, Liu JZ. Cell-free biosynthesis of chlorogenic acid using a mixture of chassis cell extracts and purified Spy-cyclized enzymes. J Agric Food Chem 2021;69:7938–47. https://doi.org/10.1021/acs.jafc.1c03309.

[13] Cha MN, Kim HJ, Kim BG, Ahn JH. Synthesis of chlorogenic acid and *p*-coumaroyl shikimates from glucose using engineered *Escherichia coli*. J Microbiol Biotechnol 2014;24:1109–17. https://doi.org/10.4014/jmb.1403.03033.

[14] Wang L, Wang H, Chen J, Hu M, Shan X, Zhou J. Efficient production of chlorogenic acid in *Escherichia coli* via modular pathway and cofactor engineering. J Agric Food Chem 2023;71:15204–12. https://doi.org/10.1021/acs.jafc.3c04419.

[15] Xiao F, Lian J, Tu S, Xie L, Li J, Zhang F, et al. Metabolic engineering of *Saccharomyces cerevisiae* for high-level production of chlorogenic acid from glucose. ACS Synth Biol 2022;11:800–11. https://doi.org/10.1021/acssynbio.1c00487.

[16] Krivoruchko A, Nielsen J. Production of natural products through metabolic engineering of *Saccharomyces cerevisiae*. Curr Opin Biotechnol 2015;35:7–15. https://doi.org/10.1016/j.copbio.2014.12.004.

[17] Borodina I, Nielsen J. Advances in metabolic engineering of yeast *Saccharomyces cerevisiae* for production of chemicals. Biotechnol J 2014;9:609–20. https://doi.org/10.1002/biot.201300445.

[18] Lian J, Mishra S, Zhao H. Recent advances in metabolic engineering of *Saccharomyces cerevisiae*: new tools and their applications. Metab Eng 2018;50:85–108. https://doi.org/10.1016/j.ymben.2018.04.011.

[19] Suástegui M, Guo W, Feng X, Shao Z. Investigating strain dependency in the production of aromatic compounds in *Saccharomyces cerevisiae*. Biotechnol Bioeng 2016;113:2676–85. https://doi.org/10.1002/bit.26037.

[20] Hassing EJ, de Groot PA, Marquenie VR, Pronk JT, Daran JMG. Connecting central carbon and aromatic amino acid metabolisms to improve de novo 2-phenylethanol production in *Saccharomyces cerevisiae*. Metab Eng 2019;56:165–80. https://doi.org/10.1016/j.ymben.2019.09.011.

[21] Pearsall SM, Rowley CN, Berry A. Advances in pathway engineering for natural product biosynthesis. ChemCatChem 2015;7:3078–93. https://doi.org/10.1002/cctc.201500602.

[22] Schulz V, Freibert SA, Boss L, Mühlenhoff U, Stehling O, Lill R. Mitochondrial [2Fe-2S] ferredoxins: new functions for old dogs. FEBS Lett 2023;597:102–21. https://doi.org/10.1002/1873-3468.14546.

[23] Kim JE, Jang IS, Son SH, Ko YJ, Cho BK, Kim SC, et al. Tailoring the *Saccharomyces cerevisiae* endoplasmic reticulum for functional assembly of terpene synthesis pathway. Metab Eng 2019;56:50–9. https://doi.org/10.1016/j.ymben.2019.08.013.

[24] Chen R, Gao J, Yu W, Chen X, Zhai X, Chen Y, et al. Engineering cofactor supply and recycling to drive phenolic acid biosynthesis in yeast. Nat Chem Biol 2022;18:520–9. https://doi.org/10.1038/s41589-022-01014-6.

[25] Cheng Y, Luo L, Tang H, Wang J, Ren L, Cui G, et al. Engineering the microenvironment of P450s to enhance the production of diterpenoids in *Saccharomyces cerevisiae*. Acta Pharm Sin B 2024:1–11. https://doi.org/10.1016/j.apsb.2024.05.019.

[26] Wu S, Chen W, Lu S, Zhang H, Yin L. Metabolic engineering of shikimic acid biosynthesis pathway for the production of shikimic acid and its branched products in microorganisms: advances and prospects. Molecules 2022;27. https://doi.org/10.3390/molecules27154779.

[27] Gibson DG, Young L, Chuang R-Y, Venter JC, Hutchison CA, Smith HO. Enzymatic assembly of DNA molecules up to several hundred kilobases. Nat Methods 2009;6:343–5. https://doi.org/10.1038/nmeth.1318.

[28] Zheng L, Baumann U, Reymond JL. An efficient one-step site-directed and site-saturation mutagenesis protocol. Nucleic Acids Res 2004;32:e115. https://doi.org/10.1093/nar/gnh110.

[29] Lee D, Lloyd NDR, Pretorius IS, Borneman AR. Heterologous production of raspberry ketone in the wine yeast *Saccharomyces cerevisiae* via pathway engineering and synthetic enzyme fusion. Microb Cell Fact 2016;15:49. https://doi.org/10.1186/s12934-016-0446-2.

[30] Stovicek V, Borodina I, Forster J. CRISPR-Cas system enables fast and simple genome editing of industrial *Saccharomyces cerevisiae* strains. Metab Eng Commun 2015;2:13–22. https://doi.org/10.1016/j.meteno.2015.03.001.

[31] Labun K, Montague TG, Gagnon JA, Thyme SB, Valen E. CHOPCHOP v2: a web tool for the next generation of CRISPR genome engineering. Nucleic Acids Res 2016;44:W272–6. https://doi.org/10.1093/NAR/GKW398.

[32] Lian J, Bao Z, Hu S, Zhao H. Engineered CRISPR/Cas9 system for multiplex genome engineering of polyploid industrial yeast strains. Biotechnol Bioeng 2018;115:1630–5. https://doi.org/10.1002/bit.26569.

[33] Tu S, Xiao F, Mei C, Li S, Qiao P, Huang Z, et al. De novo biosynthesis of sakuranetin from glucose by engineered *Saccharomyces cerevisiae*. Appl Microbiol Biotechnol 2023;107:3899–909. https://doi.org/10.1007/s00253-023-12564-7.

[34] Gietz RD. Yeast transformation by the LiAc/SS carrier DNA/PEG method. Methods Mol Biol 2014;1163:33–44. https://doi.org/10.1007/978-1-4939-1363-3_1.

[35] Verduyn C, Postma E, Scheffers WA, Van Dijken JP. Effect of benzoic acid on metabolic fluxes in yeasts: a continuous-culture study on the regulation of respiration and alcoholic fermentation. Yeast 1992;8:501–17. https://doi.org/10.1002/yea.320080703.

[36] Shang Y, Zhang P, Wei W, Li J, Ye B-C. Metabolic engineering for the high-yield production of polydatin in *Yarrowia lipolytica*. Bioresour Technol 2023;381:129129. https://doi.org/10.1016/j.biortech.2023.129129.

[37] Liu Q, Yu T, Li X, Chen Y, Campbell K, Nielsen J, et al. Rewiring carbon metabolism in yeast for high level production of aromatic chemicals. Nat Commun 2019;10:4976. https://doi.org/10.1038/s41467-019-12961-5.

[38] Kwak S, Yun EJ, Lane S, Oh EJ, Kim KH, Jin YS. Redirection of the glycolytic flux enhances isoprenoid production in *Saccharomyces cerevisiae*. Biotechnol J 2020;15:1–10. https://doi.org/10.1002/biot.201900173.

[39] Cui D, Zhang Y, Xu J, Zhang C, Li W, Xiao D. PGK1 promoter library for the regulation of acetate ester production in *Saccharomyces cerevisiae* during Chinese Baijiu fermentation. J Agric Food Chem 2018;66:7417–27. https://doi.org/10.1021/acs.jafc.8b02114.

[40] Hengardi MT, Liang C, Madivannan K, Yang LK, Koduru L, Kanagasundaram Y, et al. Reversing the directionality of reactions between non-oxidative pentose phosphate pathway and glycolytic pathway boosts mycosporine-like amino acid production in *Saccharomyces cerevisiae*. Microb Cell Fact 2024;23:121. https://doi.org/10.1186/s12934-024-02365-6.

[41] Kim SR, Xu H, Lesmana A, Kuzmanovic U, Au M, Florencia C, et al. Deletion of *PHO13*, encoding haloacid dehalogenase type IIA phosphatase, results in upregulation of the pentose phosphate pathway in *Saccharomyces cerevisiae*. Appl Environ Microbiol 2015;81:1601–9. https://doi.org/10.1128/AEM.03474-14.

[42] Qin N, Li L, Ji X, Pereira R, Chen Y, Yin S, et al. Flux regulation through glycolysis and respiration is balanced by inositol pyrophosphates in yeast. Cell 2023;186:748–763.e15. https://doi.org/10.1016/j.cell.2023.01.014.

[43] Kwak S, Yun EJ, Lane S, Oh EJ, Kim KH, Jin Y. Redirection of the glycolytic flux enhances isoprenoid production in *Saccharomyces cerevisiae*. Biotechnol J 2020;15:e1900173. https://doi.org/10.1002/biot.201900173.

[44] Bergman A, Hellgren J, Moritz T, Siewers V, Nielsen J, Chen Y. Heterologous phosphoketolase expression redirects flux towards acetate, perturbs sugar phosphate pools and increases respiratory demand in *Saccharomyces cerevisiae*. Microb Cell Fact 2019;18:25. https://doi.org/10.1186/s12934-019-1072-6.

[45] Li M, Kildegaard KR, Chen Y, Rodriguez A, Borodina I, Nielsen J. De novo production of resveratrol from glucose or ethanol by engineered *Saccharomyces cerevisiae*. Metab Eng 2015;32:1–11. https://doi.org/10.1016/j.ymben.2015.08.007.

[46] Vannelli T, Wei Qi W, Sweigard J, Gatenby AA, Sariaslani FS. Production of p-hydroxycinnamic acid from glucose in Saccharomyces cerevisiae and Escherichia coli by expression of heterologous genes from plants and fungi. Metab Eng 2007;9:142–51. https://doi.org/10.1016/j.ymben.2006.11.001.

[47] Liu H, Xiao Q, Wu X, Ma H, Li J, Guo X, et al. Mechanistic investigation of a D to N mutation in DAHP synthase that dictates carbon flux into the shikimate pathway in yeast. Commun Chem 2023;6:152. https://doi.org/10.1038/s42004-023-00946-x.

[48] Zhu J, An T, Zha W, Gao K, Li T, Zi J. Manipulation of IME4 expression, a global regulation strategy for metabolic engineering in *Saccharomyces cerevisiae*. Acta Pharm Sin B 2023;13:2795–806. https://doi.org/10.1016/j.apsb.2023.01.002.

[49] Bensen ES, Yeung BG, Payne GS. Ric1p and the Ypt6p GTPase function in a common pathway required for localization of trans-Golgi network membrane proteins. Mol Biol Cell 2001;12:13–26. https://doi.org/10.1091/mbc.12.1.13.

[50] Mukai N, Masaki K, Fujii T, Kawamukai M, Iefuji H. *PAD1* and *FDC1* are essential for the decarboxylation of phenylacrylic acids in *Saccharomyces cerevisiae*. J Biosci Bioeng 2010;109(6):564–9. https://doi.org/10.1016/j.jbiosc.2009.11.011.

[51] Siu KH, Chen RP, Sun Q, Chen L, Tsai SL, Chen W. Synthetic scaffolds for pathway enhancement. Curr Opin Biotechnol 2015;36:98–106. https://doi.org/10.1016/j.copbio.2015.08.009.
[52] Albertsen L, Chen Y, Bach LS, Rattleff S, Maury J, Brix S, et al. Diversion of flux toward sesquiterpene production in *Saccharomyces cerevisiae* by fusion of host and heterologous enzymes. Appl Environ Microbiol 2011;77:1033–40. https://doi.org/10.1128/AEM.01361-10.
[53] Liu Q, Liu Y, Li G, Savolainen O, Chen Y, Nielsen J. De novo biosynthesis of bioactive isoflavonoids by engineered yeast cell factories. Nat Commun 2021;12(1):6085. https://doi.org/10.1038/s41467-021-26361-1.
[54] Li H, Ma W, Wang W, Gao S, Shan X, Zhou J. Synergetic engineering of multiple pathways for de novo (2S)-Naringenin biosynthesis in *Saccharomyces cerevisiae*. ACS Sustainable Chem Eng 2024;12:59–71. https://doi.org/10.1021/acssuschemeng.3c04761.
[55] Shang Y, Huang S. Engineering plant cytochrome P450s for enhanced synthesis of natural products: past achievements and future perspectives. Plant Commun 2019;1:100012. https://doi.org/10.1016/j.xplc.2019.100012.
[56] Kim J-E, Jang I-S, Son S-H, Ko Y-J, Cho B-K, Kim SC, et al. Tailoring the *Saccharomyces cerevisiae* endoplasmic reticulum for functional assembly of terpene synthesis pathway. Metab Eng 2019;56:50–9. https://doi.org/10.1016/j.ymben.2019.08.013.
[57] Arendt P, Miettinen K, Pollier J, De Rycke R, Callewaert N, Goossens A. An endoplasmic reticulum-engineered yeast platform for overproduction of triterpenoids. Metab Eng 2017;40:165–75. https://doi.org/10.1016/j.ymben.2017.02.007.
[58] Ishchuk OP, Domenzain I, Sánchez BJ, Muñiz-Paredes F, Martínez JL, Nielsen J, et al. Genome-scale modeling drives 70-fold improvement of intracellular heme production in *Saccharomyces cerevisiae*. Proc Natl Acad Sci U S A 2022;119. https://doi.org/10.1073/pnas.2108245119.
[59] Zhang T, Bu P, Zeng J, Vancura A. Increased heme synthesis in yeast induces a metabolic switch from fermentation to respiration even under conditions of glucose repression. J Biol Chem 2017;292:16942–54. https://doi.org/10.1074/jbc.M117.790923.
[60] Hoffman M, Góra M, Rytka J. Identification of rate-limiting steps in yeast heme biosynthesis. Biochem Biophys Res Commun 2003;310:1247–53. https://doi.org/10.1016/j.bbrc.2003.09.151.
[61] Pereira R, Mohamed ET, Radi MS, Herrgård MJ, Feist AM, Nielsen J, et al. Elucidating aromatic acid tolerance at low pH in *Saccharomyces cerevisiae* using adaptive laboratory evolution. Proc Natl Acad Sci U S A 2020;117:27954–61. https://doi.org/10.1073/pnas.2013044117.
[62] Wang M, Toda K, Block A, Maeda HA. TAT1 and TAT2 tyrosine aminotransferases have both distinct and shared functions in tyrosine metabolism and degradation in *Arabidopsis thaliana*. J Biol Chem 2019;294:3563–76. https://doi.org/10.1074/jbc.RA118.006539.
[63] Shi W, Li J, Chen Y, Liu X, Chen Y, Guo X, et al. Metabolic engineering of *Saccharomyces cerevisiae* for ethyl acetate biosynthesis. ACS Synth Biol 2021;10:495–504. https://doi.org/10.1021/acssynbio.0c00446.
[64] Miao M, Xiang L. Pharmacological action and potential targets of chlorogenic acid. Adv Pharmacol 2020;87:71–88. https://doi.org/10.1016/bs.apha.2019.12.002.
[65] Partow S, Siewers V, Bjørn S, Nielsen J, Maury J. Characterization of different promoters for designing a new expression vector in *Saccharomyces cerevisiae*. Yeast 2010 Nov;27(11):955–64. https://doi.org/10.1002/yea.1806.
[66] Bergman A, Siewers V, Nielsen J, Chen Y. Functional expression and evaluation of heterologous phosphoketolases in *Saccharomyces cerevisiae*. AMB Express 2016;6(1):115. https://doi.org/10.1186/s13568-016-0290-0.
[67] Hinchen DJ, DuBois JL, McGeehan JE, Eltis LD. Cytochromes P450 in the biocatalytic valorization of lignin. Curr Opin Biotechnol 2022;73:43–50. https://doi.org/10.1016/j.copbio.2021.06.022.
[68] Zuo Y, Zhao M, Gou Y, Huang L, Xu Z, Lian J. Transportation engineering for enhanced production of plant natural products in microbial cell factories. Synth Syst Biotechnol 2024;9(4):742–51. https://doi.org/10.1016/j.synbio.2024.05.014.